Biodegradation (2011) 22:719–728
DOI 10.1007/s10532-010-9449-6

ORIGINAL PAPER

Characterisation of the initial degradation stage of Scots pine (*Pinus sylvestris* L.) sapwood after attack by brown-rot fungus *Coniophora puteana*

Ilze Irbe · Ingeborga Andersone · Bruno Andersons · Guna Noldt · Tatiana Dizhbite · Nina Kurnosova · Mari Nuopponen · Derek Stewart

Received: 20 April 2010 / Accepted: 24 December 2010 / Published online: 16 February 2011

Abstract In our study, early period degradation (10 days) of Scots pine (*Pinus sylvestris* L.) sapwood by the brown-rot fungus *Coniophora puteana* (Schum.: Fr.) Karst. (BAM Ebw.15) was followed at the wood chemical composition and ultrastructure-level, and highlighted the generation of reactive oxygen species (ROS). An advanced decay period of 50 days was chosen for comparison of the degradation dynamics. Scanning UV microspectrophotometry (UMSP) analyses of lignin distribution in wood cells revealed that the linkages of lignin and polysaccharides were already disrupted in the early period of fungal attack. An increase in the lignin absorption A_{280} value from 0.24 (control) to 0.44 in decayed wood was attributed to its oxidative modification which has been proposed to be generated by Fenton reaction derived ROS. The wood weight loss in the initial degradation period was 2%, whilst cellulose and lignin content decreased by 6.7% and 1%, respectively. Lignin methoxyl ($-OCH_3$) content decreased from 15.1% (control) to 14.2% in decayed wood. Diffuse reflectance Fourier-transform infrared (DRIFT) spectroscopy corroborated the moderate loss in the hemicellulose and lignin degradation accompanying degradation. Electron paramagnetic resonance spectra and spin trapping confirmed the generation of ROS, such as hydroxyl radicals ($HO^{\bullet}$), in the early wood degradation period. Our results showed that irreversible changes in wood structure started immediately after wood colonisation by fungal hyphae and the results generated here will assist in the understanding of the biochemical mechanisms of wood biodegradation by brown-rot fungi with the ultimate aim of developing novel wood protection methods.

Keywords *Coniophora puteana* · Brown-rot · Scots pine · Early degradation · ROS · Wood components

I. Irbe (✉) · I. Andersone · B. Andersons · T. Dizhbite · N. Kurnosova
Latvian State Institute of Wood Chemistry, Dzerbenes Str. 27, Riga LV-1006, Latvia
e-mail: ilzeirbe@edi.lv

G. Noldt
Division of Wood Biology, Department of Wood Science, Hamburg University, Leuschnerstrasse 91, 21031 Hamburg, Germany

M. Nuopponen · D. Stewart
Scottish Crop Research Institute, Plant Products and Food Quality Programme, Dundee DD2 5DA, Scotland, UK

Introduction

Although studied for some time, the mechanisms of wood biodegradation by brown-rot fungi are yet not fully understood. The dynamics of biodegradation from early to late degradation stages as well as the critical stage in the degradation period, which causes irreversible consequences in the wood structure, are unclear. Many factors have hindered progress, in

particular, the complexity of the wood substrate and the multiplicity of produced enzymes. Brown-rot fungi cause an extensive degradation of holocellulose in wood, whilst the lignin fraction is mainly demethylated and depolymerized (Goodell et al. 2003; Eriksson et al. 1990; Schmidt 2006) often leading to lignin-derived volatile components (Ewen et al. 2004). Current results indicate that wood-rotting fungi possess two independent types of systems capable of internal scission of cellulose molecules—enzymatic and radical-based ones. Degradation of cellulose by cellulolytic enzymes would be expected to produce a localized superficial attack because the cellulases are too large to penetrate the microstructure of cellulose (Flournoy et al. 1991; Baldrian and Valaskova 2008). It has been proposed that brown-rot fungi employ Fenton chemistry (H_2O_2–Fe(II)) to generate hydroxyl radicals (HȮ) which initiate lignocellulose breakdown (Contreras et al. 2007; Suzuki et al. 2006; Kaneko et al. 2005; Kim et al. 2002; Cohen et al. 2002; Kramer et al. 2004). Consequently, this suggests that reactive oxygen species (ROS) play an important role in the early wood degradation by brown-rot fungi.

In the present study, the investigation was mainly focussed on the early period of wood degradation, as this is considered to be a critical step for significant reduction in strength properties (Clausen and Kartal 2003). Initial degradation of Scots pine (*Pinus sylvestris* L.) sapwood was characterized and compared with the later wood degradation period by applying different and complementary chemical and physical analytical methods.

Materials and methods

Wood decay test

Scots pine (*Pinus sylvestris* L.) sapwood blocks ($20 \times 20 \times 5$ mm^3) with seven to ten annual growth rings per 10 mm were exposed to the brown-rot fungus *Coniophora puteana* (Schum.: Fr.) Karst. (BAM Ebw.15) on a medium containing 5% malt extract concentrate and 3% Fluka agar (*BioChemika*) in Kolle flasks. The test procedures of the European standard EN 113 (2000) were followed. Sterile wood blocks with the largest face (cross section) were aseptically placed on 3-mm stainless steel supports and incubated at 22°C and 70% relative humidity for 10 (early degradation) to 50 (late degradation) days. Three replicates for each test period were taken. Subsequent to cultivation, the blocks were removed from the culture vessels, brushed free of mycelium and oven dried at 103°C for 5 h. The weight loss (%) was calculated from the dry weight before and after the test.

Determination of cellulose and lignin content

Wood components were determined in control wood blocks and those following fungal exposure for 10 and 50 days. Cellulose was determined using the Kürschner–Hoffer method. Briefly, wood meal (1 g) was refluxed for 1 h with an alcoholic solution of nitric acid (100 ml ethanol and 25 ml concentrated nitric acid). The residue was filtered off and refluxed as before. The procedure was repeated three to four times. Finally, the residue was washed with alcoholic nitric acid then water, dried at 105°C and weighed (Browning 1967). Lignin was determined using 72% sulphuric acid (Klason method). Briefly, wood meal (1 g) was treated with 15 ml 72% sulphuric acid. After standing for 2 h at 25°C with occasional stirring, the mixture was diluted with 200 ml distilled water and heated to reflux for 1 h. The lignin was then filtered, washed free of acid, dried at 105°C, and weighed (Browning 1967). Furthermore, lignin methoxyl ($-OCH_3$) group content was determined according to the TAPPI method (Zakis 1994).

Diffuse reflectance Fourier-transform infrared (DRIFT) spectroscopy

Samples of control wood (0 days) and early (10 days) and late (50 days) fungi-degraded wood were washed with water, dried at 50°C for 4 days and hammer-milled to pass a 0.5 mm sieve. The samples were then analysed by Diffuse reflectance Fourier-transform infrared (DRIFT) spectroscopy as described by Nuopponen et al. (2006).

Scanning UV microspectrophotometry (UMSP)

Small wood sticks (5 mm in the longitudinal direction) were cut off the dry wood blocks decayed for 10 and 50 days. The sticks were dehydrated in acetone, impregnated with Spurr's epoxy resin (Spurr 1969)

through a series of acetone/resin mixtures, followed by immersion in pure resin and polymerisation at 70°C for 24 h. The embedded samples were trimmed to provide a face of approximately 0.5 mm^2. Ultrathin sections (1 μm) were cut with a diamond knife mounted in an LKB Bromma ultramicrotome. The sections were transferred to quartz microscope slides, immersed in a drop of non-UV-absorbing glycerine, covered with a quartz cover slip and observed with objective lenses of 32:1 and 100:1. An immersion oil of glycerine/water mixture $n_D = 1.46$ was used.

Analyses were carried out on a Zeiss-UMSP 80 instrument equipped with a scanning stage to allow the determination of image profiles at constant wavelengths (e.g. 280 nm) using the scan programme APAMOS (automatic photometric analysis of microscopic objects by scanning, Zeiss). The scan programme digitises rectangular fields of the tissue with a local geometric resolution of 0.25 μm × 0.25 μm and a photometric resolution of 4096 greyscale levels, which are converted into 14 basic colours to visualise the absorbance intensities (Koch and Kleist 2001).

The UV absorbance of the lignified cell walls in tissues was measured by point analysis of 1 μm^2 over the wavelength range 240–400 nm using the programme LAMWIN (Zeiss) (Koch and Grünwald 2004).

The late- and earlywood cells were analysed by both scanning and point measurements. For point analysis, the secondary wall of each tracheid was measured in three different positions. A total of 60 point measurements for controls and each decay period were obtained. The most characteristic UV spectra were chosen for illustration of the decay pattern.

Electron paramagnetic resonance (EPR) spectroscopy

EPR spin-trapping techniques using nitrone 5,5-dimethyl-1-pyrroline-N-oxide (DMPO) as spin trap was employed to identify and tentatively quantify the free radical intermediates in wood samples after 10 and 30 days of fungal degradation. EPR spectra were recorded at room temperature using a computer-controlled BRUKER EMX system operating at a frequency of 9 GHz (X-band) and power of 10 mW. The instrument settings used were: modulation frequency at 100 kHz, modulation amplitude at 0.1 mT, time constant at 0.16 s, field set at 334.0 mT G, scan range at 10 or 20 mT, scan time 4 min, and receiver gain at 10×10^5 or 10×10^6. The various components of EPR parameters (g-value, hyperfine splitting α and line width) were determined directly from the spectra. Spin trapping procedure for wood samples was as follows: a few fresh matchsticks like samples (1 × 1 × 5 mm) were cut from each wood block and soaked for 2.5 min in an aqueous solution of 200 mM DMPO, then transferred to a quartz EPR tube with 4.5 mm inner diameter. The bottom of the EPR tube was sealed and the tube inserted into the sample cavity of the spectrometer. A summary of the steps prior to EPR measurements are shown in Fig. 1. Measurements were taken immediately after the instrument was tuned and completed within 20 min after the DMPO came into contact with the wood.

The integral intensities of EPR spectra were obtained by evaluating their double integrals (DI_{EPR}) using the WIN EPR software (Bruker). The relative concentration (c_{rel}) of paramagnetic species were calculated as $c_{rel} = DI_{EPR}/DI_{EPR}^{ref}$, where DI_{EPR} and DI_{EPR}^{ref} represent double integrals found for wood samples and reference samples, respectively. The monocrystal of Cr^{3+} within MgO matrix (about 0.5×10^{13} spins) was used as an internal reference sample for tentative quantifying of DMPO/OH adduct content of the wood samples, whereas weak pitch sample, which was supplied by Bruker and contained 1×10^{13} of spins per 1 cm, was used for calculation of lignin related free radicals.

DMPO was purchased from Sigma-Aldrich; the aqueous solutions were made up in Milli-Q-filtered (Millipore) water. DMPO samples by themselves, without any addition, showed no EPR signal.

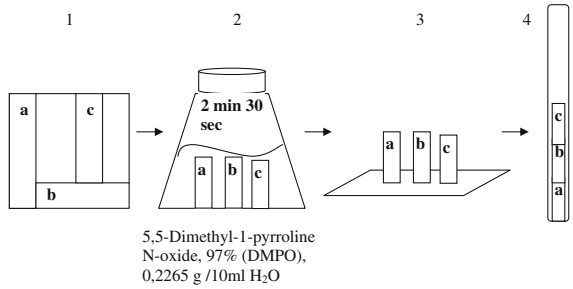

Fig. 1 Fresh matchstick like samples (*1*) were cut from each wood sample and soaked in solution of DMPO (*2*), then surface-dried with filter paper (*3*) and transferred to the EPR tube (*4*)

Results and discussion

Content of cellulose, lignin and methoxyl groups

Changes in wood components during decay by brown-rot fungus *Coniophora puteana* are shown in Table 1. Weight loss, as well cellulose and lignin content, were minimal in the initial degradation period. However, the decrease in the lignin methoxyl groups was significant in the early degradation stage, dropping by 6% from 15.1 to 14.2%. As a comparison to highlight the degradation dynamics, the late fungal exposure period of 50 days was chosen and this exhibited a drastic increase of weight loss (55%) based on cellulose depletion (17%) and relative growth of lignin content to 59.7%. In addition the late degradation period was accompanied by a further decrease in methoxyl content (down $\sim$20% of the control value). The oxidative demethylation in brown-rotted wood comprised the removal of the methyl (CH_3–) groups from the aryl-methoxyl portion and promoted the formation of reactive hydroxyl groups (Fig. 5). Our results corroborate those of Yelle et al. (2008) who reported cleavage of lignin by a brown-rot fungus *Gloeophyllum trabeum* in extensively degraded spruce wood with an accompanying weight loss of 64% after 16 weeks exposure. The authors report that besides lignin demethoxylation, a non-selective depletion of all intermonomer side-chain linkages occurred and suggested that the resulting aromatic polymer was probably interconnected by new linkages that lack hydrogens and was no longer recognizable as lignin.

However, the role of lignin degrading enzymes in some brown-rot fungi cannot be excluded and it has been reported (Lee et al. 2004) that the brown-rot fungus *Coniophora puteana* produces laccase with the maximum activity after 3–5 days of incubation. To summarise, we suppose that both factors, non-enzymatic and enzymatic, play an important role in degradation of polysaccharides and lignin by brown-rot fungi.

DRIFT results

Analysis by DRIFT spectroscopy corroborated recent FT-IR related insights (Martin et al. 2005; Popescu et al. 2010) into the fungal-associated (in particular brown rot; Fackler et al. 2010) changes in the wood macrochemistry and highlights changes that corroborate with the progressive weight loss found here (Fig. 2). The progressive and preferential degradation of the polysaccharide component, highlighted by the relative reduction in the glucomannan- and/or xylan-derived ester carbonyl absorbance at $\sim$1730 cm^{-1} and a sharpening of the structural polysaccharide absorbances at 1100–1000 cm^{-1}, and consequential proportional increase in lignin is reflected in a sharpening of the lignin-related absorbances at 1508 (C=C stretch) and 1262 cm^{-1} (guaiacyl ring and C–O stretch). In addition, although these changes were most intense for the sample exposed for 50 days they were in evidence at earlier stages (10 days) where weight loss was minimal and this matches the FT-IR-monitored brown rot decay pattern in spruce (Fackler et al. 2010) and beech and pine (Weiland and Guyonnet 2003). Furthermore, the carbonyl bands over the region 1680–1630 cm^{-1} increased in intensity as the decay progressed. Although classically a region of pectic absorbances, these polysaccharides, situated in the middle lamellae, are general removed in the initial stages of fungal degradation (Blanchette and Abad 1988; Popescu et al. 2010) meaning that this observed absorbance increase supports the proposed oxidative degradation and the consequential generation of phenyl carbonyl structures (Ph–CO–, Faix 1991; Popescu et al. 2010) in the residual lignin.

Table 1 Changes in cellulose, lignin and methoxyl content of pine wood (*Pinus sylvestris*) following exposure to the brown-rot fungus *C. puteana*

Degradation time (days)	Weight loss (%)	Cellulose* (w/w %)	Lignin* (w/w %)	Methoxyl groups* (%)
Control	–	53.9	31.3	15.1
10	2 ± 1	50.3	31.0	14.2
50	55 ± 1	17.0	59.7	12.1

* Standard error of the mean (SEM) <1%: $n = 3$

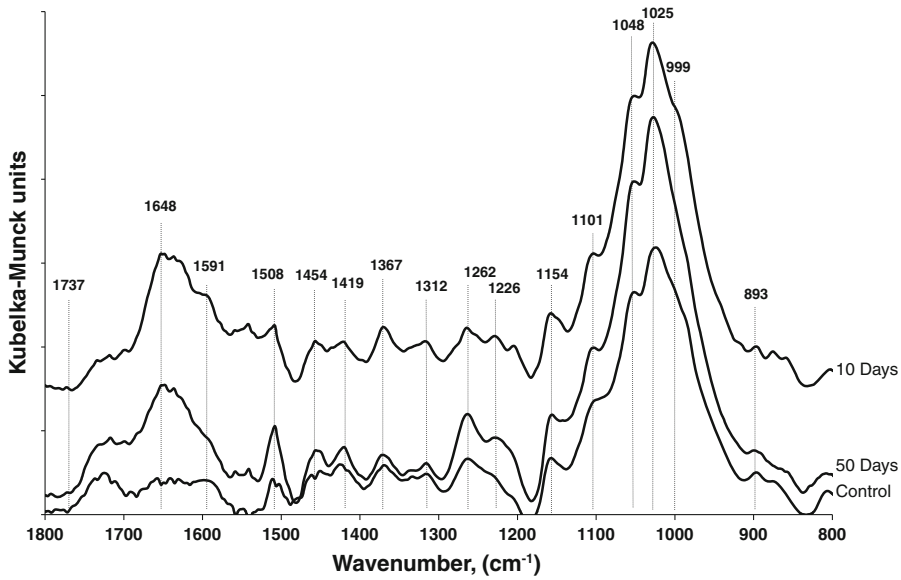

Fig. 2 DRIFT spectra of pine wood control and *C. puteana* degraded wood

UV microspectrophotometry

a. Point analysis

UV micropspectrophotometric analysis of the latewood cell walls (Fig. 3) illustrate the changes in lignin quantity with respect to polysaccharides. Figure 3 shows the characteristic spectra of the control (A_{280nm} 0.24) and the following decay periods, measured in S_2 layer. Relative lignin concentration increased gradually in the fungally degraded S_2 as the polysaccharides were preferably degraded (Table 1). After 10 days the A_{280nm} was elevated to 0.44, while in late degradation of 50 days absorbance value of 0.52 was observed.

The apparent lignin concentration increased in early decay period (10 days exposure) though the corresponding wood weight loss was negligible (Table 1). An extracellular HȮ production (Fig. 5) may contribute to initial depolymerization of polysaccharides, without enzymes, which cannot penetrate the narrow pores of wood, and thus no enzymatic metabolism takes place that could lead to weight loss.

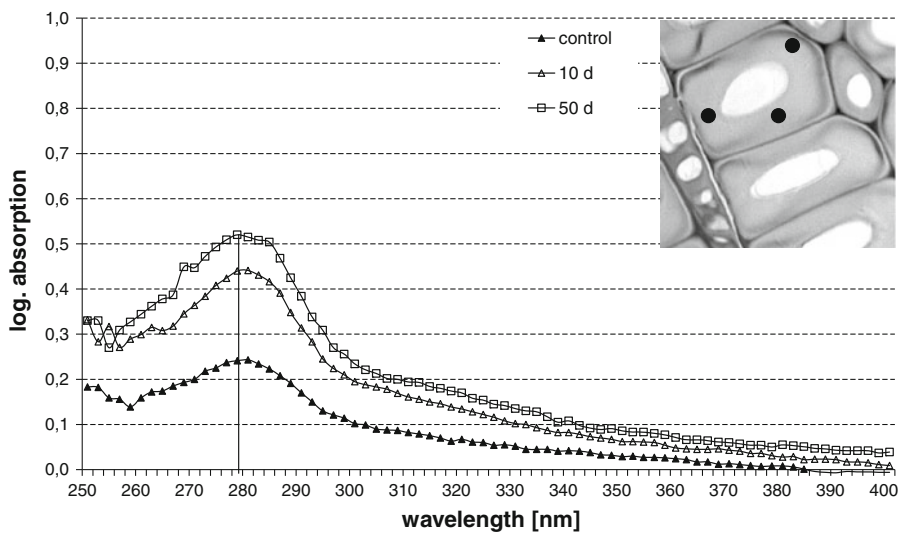

Fig. 3 Lignin absorbance spectra of latewood in control and decayed tracheids. Inserted UV photograph of latewood control identifies the measurement spots in each cell (*black dots*) (100×)

It is not surprising that the lignin moiety is also subjected to oxidative changes in the presence of nascent ROS. It is possible that the early increase in A_{280nm} is mainly a manifestation of oxidative lignin modification. Highley and Dashek (1998) reported that brown-rot fungi, similarly to white rots, demethylate methoxyl groups in phenolic and non-phenolic lignin structures, hydroxylate aromatic rings, and promote side-chain oxidations and aromatic ring-cleavage reactions. All these structural modifications lead to an increase in absorbance at 280 nm. It is also possible that linkages between lignin and polysaccharides are oxidatively cleaved, especially in the case of ester linkages, which can be cleaved at low pH thereby adding to the phenolic moieties absorbing at 280 nm.

In toto, the increase in absorbance (A_{280nm}) is probably due to increment in lignin concentration (Table 1) and the ROS-driven oxidative changes. The is supported by the data for the material that experienced 50 days of exposure (Fig. 3), which exhibited a weight loss of reached 55% suggesting

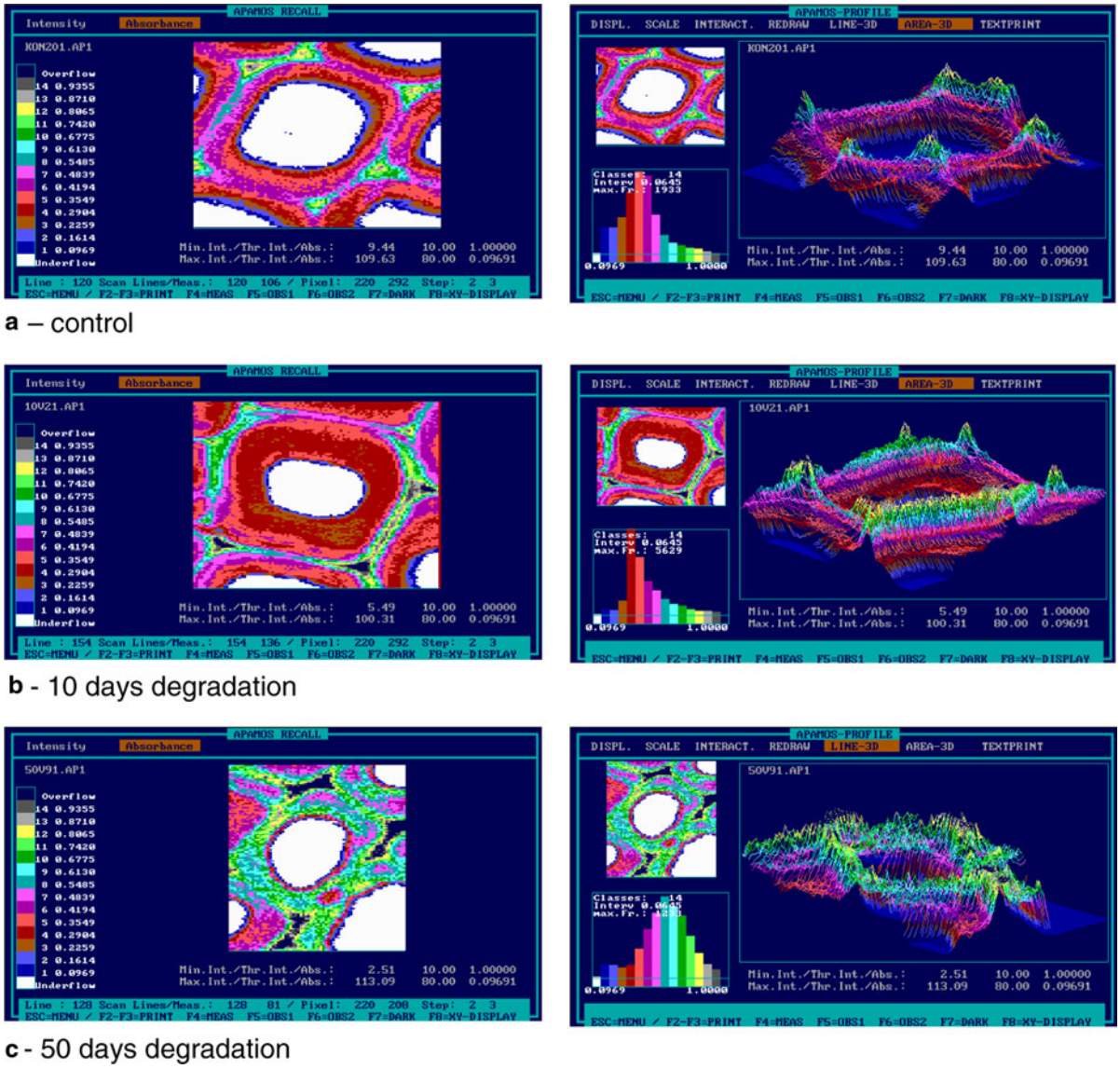

Fig. 4 UV microscopic image profiles of **a** control pine latewood tracheids and **b** 10 days and and **c** 50 days tracheids degraded by the brown rot fungus *C. puteana*. The *colour* scale indicates the different UV-absorbance values at wavelength of λ_{280nm}

that fungal cellulases had penetrated deep into the cell wall facilitating carbohydrate degradation and removal.

b. Scanned surface profiles of lignin distribution

Figure 4 shows 2D and 3D UV images of lignin distribution in pine latewood tracheids. The pixel colours indicate different intensities of UV absorbance at 280 nm. The high resolution (0.25 μm × 0.25 μm per pixel) allowed detailed differentiation of the UV absorbance within the cell walls. The images of pine sapwood control and degraded samples were characterised by high absorbance at the compound middle lamellae (CML) and cell corners (A_{280nm} 0.61–0.93) compared to the secondary wall layers with lower lignin content (A_{280nm} 22–0.48). Scan images of the control (Fig. 4a) and slightly decayed sample (Fig. 4b) showed no significant differences in UV absorbance of the individual cell wall layers. Comparison of histograms of the UV absorbance revealed a slight decrease in the lower values represented by blue, brown and pink pixels (high to low A_{280nm}), and a slight increase in A_{280nm} 0.29 could be observed after 10 days of wood degradation. Figure 4c shows the lignin distribution in pinewood exposed to *C. puteana* for 50 days. Distinct changes in cell wall structure were observed in the advanced decay stage. The secondary wall spectra showed signs of significant alteration to the wall chemistry, which was reflected by the strong increase in UV absorbances represented by the green pixels (A_{280nm} 0.54–0.74). This corroborates the aforementioned extensive degradation of polysaccharides in the secondary wall, where remaining lignin showed high absorbance values.

EPR spectroscopy results

The proposed Fenton chemistry-based mode of degradation we tested using an EPR method. Figure 5 shows the EPR spectra of the wood sample (degradation time 10 days) before (a) and after (b, c) treatment with DMPO. In the spectra of Fig. 5b and c, the four-line adsorption pattern with an intensity ratio of 1:2:2:1 and a 1.48 mT hyperfine splitting constant (Table 2) is definitely assignable to DMPO-OH adduct (Finkelstein et al. 1980; Yoshioka et al. 1996; Robert et al. 2002). No DMPO-OH EPR signal

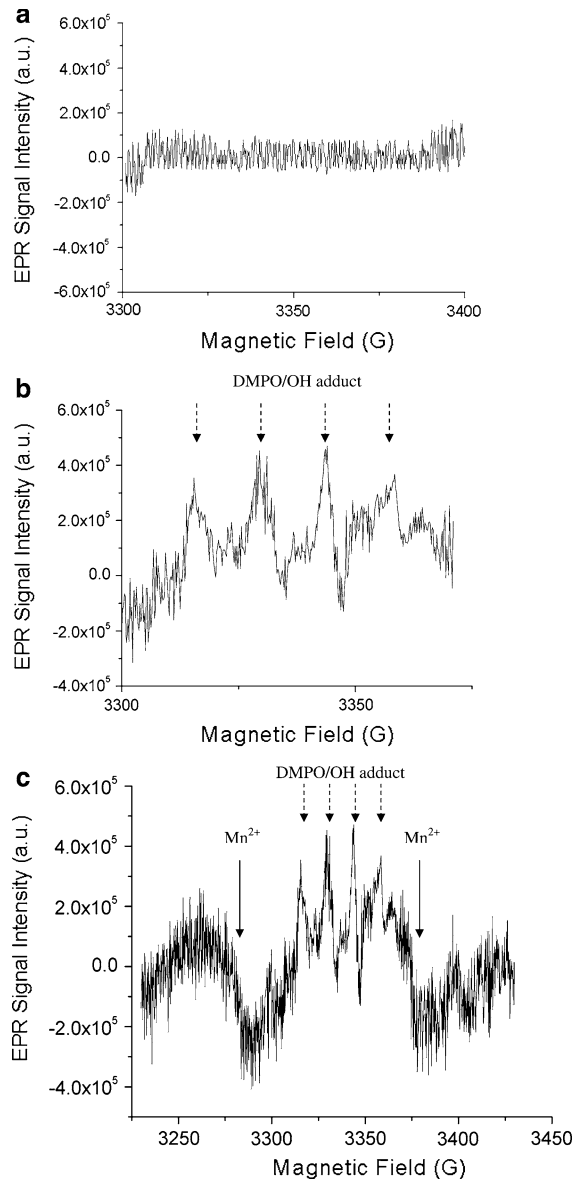

Fig. 5 EPR spectra of the wood sample (10 days after *C. puteana* degradation) **a** before and **b** and **c** after treatment with DMPO. Scan range: 100 G = 10 mT (**a** and **b**) and 200 G = 20 mT (**c**). *Black arrows* show the paramagnetic manganese signal, *dashed arrows* the DMPO/OH adduct. All spectra are the average of eight EPR signal scans

was detected in control wood sample. No four-line EPR signal was detected when DMPO has been omitted. From these results it is evident that $HO^{\bullet}$ radicals were formed in the sample during its biodegradation by brown-rot fungus *Coniophora puteana.* Using EPR approach, formation of $HO^{\bullet}$

Table 2 Paramagnetic characteristics of pine wood (*Pinus sylvestris*) following exposure to the brown-rot fungus *C. puteana* and subsequent treatment with DMPO

Degradation time (days)	EPR spectrum parameters				
	g-value	$\alpha_N = \alpha_H$, mT	ΔH_{max}, mT	DMPO/OH signal intensity, c^a_{rel}	Content of radicals caused singlet EPR spectrum, spins/g
10	2.0058 ± 0.0002	1.48 ± 0.02	0.3 ± 0.05	10.1 ± 0.5	$<1 \times 10^{16}$
30	2.0060 ± 0.0002	1.50 ± 0.02	0.3 ± 0.02	13.2 ± 0.7	$(8 \pm 1) \times 10^{16}$

[a] Intensity was calculated as ratio of integral intensities of the spectrum of DMPO/OH spin adduct to the intensity of EPR spectrum of the internal standard

radicals in situ was detected both in very early period (10 days) of wood degradation (Table 2; Fig. 5), and advanced period of 30 days, when the weight loss of pine wood reached 24% (data not shown). Previous EPR studies have demonstrated hydroxyl radical generation in liquid culture medium and during the colonization of wood slivers of Douglas fir and white fir by the brown-rot fungus *Postia placenta* for 4–5 weeks (Illman et al. 1989). Our results confirmed hydroxyl radical production in very early wood colonization by the fungal hyphae.

The EPR spectrum provided by DMPO/OH adduct appeared on a shoulder (Fig. 5c) of one of the hyperfine lines of the paramagnetic manganese signal. The signal was detected due to the relative closeness of g-values for Mn^{2+} and adduct. The question arises, if the $Mn^{2+}$is related to the process of wood biodegradation, because similar Mn^{2+} signal was observed in the EPR spectra of control wood not degraded by the fungus. The source of Mn^{2+} during the deterioration process is discussed by Illman et al. (1989). The authors suppose that the Mn^{3+} typically found in wood could be catalyzing the hydrogen peroxide generation of $OH^{\bullet}$ or Mn^{2+} EPR detectable signals could be masked by chemical binding that is changed during fungal colonization. The chemical changes could result in $OH^{\bullet}$ production.

Iron, a typical transition metal in Fenton-based reactions, in the non-degraded wood is usually found in low concentrations. In the aerobic environment the most stable valence state for iron is the ferric rather than the ferrous state and very little iron in the reduced state would be found in natural environments (Goodell et al. 1997). Iron oxidation states were not detected in our EPR experiments as well as previous works (Illman and Bajt 1997). EPR iron signal obviously was not observed due to the reduction of Fe^{3+} to Fe^{2+}, which is EPR silent.

Comparison of EPR spectra of wood samples after various exposure periods showed that by increasing the period of biodegradation, the level of $HO^{\bullet}$ radicals in wood increased. Thus, the DMPO/OH adduct content in the wood treated with DMPO after 30 days of fungal attack was ~30% higher than that for the sample after 10 days biodegradation (Table 2).

In the EPR spectrum of 30 days decayed sample, treated with DMPO, besides the signal from DMPO/OH spin adduct (Fig. 5c), the narrow singlet spectrum with g-value about 2.0040 and a peak-to-peak width of 0.6 mT was observed (data not shown). This line was detected also for the sample in the absence of treatment with DMPO. The literature (Yoshioka et al. 2001) and our own experience (Dizhbite et al. 2004; Telysheva et al. 2007) suggests that the singlet EPR signal can be attributed to the lignin-derived radicals including semiquinone radical-anions. The content of these radicals in the wood sample with biodegradation time of 30 days was of 8×10^{16} spins/g compared to a value of $<1 \times 10^{16}$ spins/g in the control wood. The evolution of the singlet EPR signal is supportive of the homolytic destruction of lignin during biodegradation and is in line with the aforementioned literature (Yoshioka et al. 2001) and personal experience (Dizhbite et al. 2004; Telysheva et al. 2007).

We propose that one of the sources for ROS production is related to cleavage of methoxyl groups (Table 1) and formation of the reactive phenolic hydroxyl groups. It has been shown previously that ROS also can be generated via glycopeptide mechanism ((Enoki et al. 1989), cellobiose dehydrogenase (CDH) (Hyde and Wood 1997), and quinone redox cycling (Goodell et al. 1997).

Conclusion

Irreversible processes in the wood cell wall started immediately after wood colonization by the brown-rot fungus *Coniophora puteana*. Hydroxyl radical formation (EPR) in the initial stage of cell wall degradation showed a considerable relative increase in lignin-related UV absorbance (UMSP) attributed to the oxidative changes in lignin structure.

Acknowledgments The research leading to these results has partially received funding from the European Community's Seventh Framework Programme (FP7/2007-2013) under grant agreement No. 203459, and the Latvian Scientific Council grant No. 09.1600. The authors thank Dr. Gerald Koch, Federal Research Institute for Rural Areas, Forestry and Fisheries (vTI), Hamburg, for his assistance in obtaining of UMSP spectra and interpretation of results. DS acknowledges funding from Scottish Government Rural and Environment Research and Analysis Directorate (RERAD).

References

Baldrian P, Valaskova V (2008) Degradation of cellulose by basidiomycetous fungi. FEMS Microbiol Rev 32:501–521

Blanchette RA, Abad AR (1988) Ultrastructural localization of hemicellulose in birch wood (*Betula papyrifera*) decayed by brown and white rot fungi. Holzforschung 42:393–398

Browning BL (1967) Methods of wood chemistry, Vol I. Wiley, Interscience Publishers, New York

Clausen CA, Kartal SN (2003) Accelerated detection of brown-rot decay: comparison of soil block test, chemical analysis, mechanical properties, and immunodetection. For Prod J 53(11/12):90–94

Cohen R, Jensen KA Jr, Houtman CJ, Hammel KE (2002) Significant levels of extracellular reactive oxygen species produced by brown rot basidiomycetes on cellulose. FEBS Lett 531:483–488

Contreras D, Rodríguez J, Freer J, Schwederski B, Kaim W (2007) Enhanced hydroxyl radical production by dihydroxybenzene-driven Fenton reactions: implications for wood biodegradation. J Biol Inorg Chem 12:1055–1061

Dizhbite T, Telysheva G, Jurkjane V, Viesturs U (2004) Characterization of the radical scavenging activity of lignins—natural antioxidants. Bioresour Technol 95: 309–317

Enoki A, Tanaka H, Fuse G (1989) Relationship between degradation of wood and production of H_2O_2-producing or one-electron oxidases by brown-rot fungi. Wood Sci Technol 23(1):1–12

Eriksson KE, Blanchette RA, Ander P (1990) Microbial and enzymatic degradation of wood and wood components. Springer-Verlag, Berlin

European Standard EN 113 (2000) Wood preservatives. Method of test for determining the protective effectiveness against wood destroying basidiomycetes. European Committee for Standardization, CEN, Bruessels

Ewen RJ, Jones PR, Ratcliffe NM, Spencer-Phillips PT (2004) Identification by gas chromatography-mass spectrometry of the volatile organic compounds emitted from the wood-rotting fungi *Serpula lacrymans* and *Coniophora puteana*, and from *Pinus sylvestris* timber. Mycol Res 108:806–814

Fackler K, Stevanic JS, Tersa T, Hinterstoisser B, Schwanninger M, Salmén L (2010) Localisation and characterisation of incipient brown-rot decay within spruce wood cell walls using FT-IR imaging microscopy. Enzym Microb Technol 47:257–267

Faix O (1991) Classification of lignins from different botanical origins by FT-IR spectroscopy. Holzforschung 45:21–27

Finkelstein E, Rosen GM, Rauckman EJ (1980) Spin trapping, kinetics of the reaction of superoxide and hydroxyl radicals with nitrones. J Am Chem Soc 102:4994–4999

Flournoy DS, Kirk TK, Highley TL (1991) Wood decay by brown-rot fungi: changes in pore structure and cell wall volume. Holzforschung 45:383–388

Goodell B, Jellison J, Liu J, Daniel G et al (1997) Low molecular weight chelators and phenolic compounds isolated from wood decay fungi and their role in the fungal biodegradation of wood. J Biotechnol 53:133–162

Goodell B, Nicholas DD, Schultz TP (eds) (2003) Wood deterioration and preservation. Advances in our changing world. American Chemical Society (ACS), Washington, DC

Highley TL, Dashek WV (1998) Biotechnology in the study of brown- and white rot decay. In: Bruce A, Palfreyman JW (eds) Forest products, biotechnology. TJ International Ltd, UK, pp 15–36

Hyde SM, Wood PM (1997) A mechanism for production of hydroxyl radicals by the brown-rot fungus *Coniophora puteana*: Fe(III) reduction by cellobiose dehydrogenase and Fe(II) oxidation at a distance from the hyphae. J Microbiol 143:259–266

Illman BL, Bajt S (1997) Nondestructive elemental analysis of wood biodeterioration using electron paramagnetic rezonanse and synchroton X-ray fluorescence. Int Biodet Biodegrad 39(2–3):235–243

Illman BL, Meinholtz DC, Highley TL (1989) Oxygen free radical detection in wood colonized by the brown-rot fungus, *Postia placenta.* In: Biodeterioration Research 2. Plenum Press, New York, pp 497–509

Kaneko S, Yoshitake K, Itakura S, Tanaka H, Enoki A (2005) Relationship between production of hydroxyl radicals and degradation of wood, crystalline cellulose, and a lignin-related compound or accumulation of oxalic acid in cultures of brown-rot fungi. J Wood Sci 51:262–269

Kim YS, Wi SG, Lee KH, Singh AP (2002) Cytochemical localization of hydrogen peroxide production during wood decay by brown-rot fungi *Tyromyces palustris* and *Coniophora puteana*. Holzforschung 56:7–12

Koch G, Grünwald C (2004) Application of UV microspectrophotometry for the topochemical detection of lignin and phenolic extractives in wood fibre cell walls. In: COST Action E20, Wood fibre cell walls: methods to study their formation, structure and properties, pp 119–130

Koch G, Kleist G (2001) Application of scanning UV microspectrophotometry to localise lignins and phenolic extractives in plant cell walls. Holzforschung 55:563–567

Kramer C, Kreisel G, Fahr K, Kaessbohrer J, Schlosser D (2004) Degradation of 2-fluorphenol by the brown-rot fungus *Gloeophyllum striatum*: Evidence for the involvement of extracellular Fenton chemistry. Appl Microbiol Biotechnol 64:387–395

Lee KH, Wi SG, Singh AP, Kim YS (2004) Micromorphological characteristics of decayed wood and laccase produced by the brown-rot fungus *Coniophora puteana*. J Wood Sci 50:281–284

Martin JA, Solla A, Coimbra MA, Gil L (2005) Metabolic distinction of Ulmus minor xylem tissues after inoculation with *Ophiostoma novo-ulmi*. Phytochemistry 66:2458–2467

Nuopponen MH, Birch GM, Sykes RJ, Lee SJ, Stewart D (2006) Estimation of wood density and chemical composition by means of diffuse reflectance mid-infrared Fourier transform (DRIFT-MIR) spectroscopy. J Agric Food Chem 54:34

Popescu CM, Popescu MC, Vasile C (2010) Characterization of fungal degraded lime wood by FT-IR and 2D IR correlation spectroscopy. Microchem J 95:377–387

Robert R, Barbati S, Ricq N, Ambrosio M (2002) Intermediates in wet oxidation of cellulose: identification of hydroxyl radical and characterization of hydrogen peroxide. Water Res 36(19):4821–4829

Schmidt O (2006) Wood and tree fungi. Springer-Verlag, Berlin, Heidelberg

Spurr AR (1969) A low viscosity epoxy resin embedding medium for electron microscopy. J Ultrastruct Res 26:31–43

Suzuki MR, Hunt G, Houtman CJ, Dalebroux ZD, Hammel KE (2006) Fungal hydroquinones contribute to brown rot of wood. Environ Microbiol 8(12):2214–2223

Telysheva G, Dobele G, Meier D, Dizhbite T, Rossinskaja G, Jurkjane V (2007) Characterization of lignocellulosics structure transformation upon degradation in phytocenotic condition. J Anal Appl Pyrolysis 79:52–60

Weiland JJ, Guyonnet R (2003) Study of chemical modifications and fungi degradation of thermally modified wood using DRIFT spectroscopy. Holz als Roh- und Werkstoff 61:216–220

Yelle DJ, Ralph J, Lu F, Hammel KE (2008) Evidence of cleavage of lignin by a brown rot basidiomycete. Environ Microbiol 10(7):1844–1849

Yoshioka H, Yoshioka H, Hasegawa K (1996) Solid-state spin trapping of the hydroxyl radical formed by gamma-irradiation in ice and the scavenging effect of sodium L-ascorbate. Biosci Biotech Biochem 60:1971–1975

Yoshioka A, Seino T, Takai M, Tabata M (2001) Thermal induced homolytic scissions of lignin interunitary bonds in the hardwood lignin solution. An ESR study combined with a spin trapping method. J Wood Chem Technol 21(2):113–125

Zakis GF (1994) Functional analysis of lignins and their derivates. TAPPI Press, Atlanta